# Bose-Einstein condensates in deformed traps

Author: Miguel Lebón Dias
*Facultat de Física, Universitat de Barcelona, Avd. Diagonal 645, 08028 Barcelona, Spain.*

Advisor: Bruno Juliá-Díaz

**Abstract:** In this degree thesis we study the properties of a Bose-Einstein condensate confined in both isotropic and anisotropic traps using a mean-field description in terms of the Gross-Pitaevskii equation and modified Gross-Pitaevskii equation. We also study the many particle limit and compare it with the Thomas-Fermi limits. Finally we study the aspect ratio of the system and see how it changes for the noninteracting limit and the strong repulsive limit.

## I. INTRODUCTION

If we confine $N$ bosons in a trap with an external potential at low temperatures (ideally $T = 0K$) they condense in the same single particle state. This allows us to describe the system with a single wave function. This is called a Bose-Einstein condensate [1].

In the limit of a very diluted gas i.e. the average distance among particles is much larger than the range of interaction, the system is dominated by two-body interactions, well described in terms of the $s$-wave scattering length. Under these conditions an accurate description of the condensate wave function is provided by the mean-field description [2].

In this work we will solve the Gross-Pitaevskii (GP) and modified Gross-Pitaevskii (MGP) equation of a diluted gas of $^{87}$Rb approximated as a hard sphere gas in an isotropic and in an anisotropic trap [3,4]. To study it we will use the local-density approximation (LDA) based on an energy functional derived by the low-density expansion of the energy in an uniform hard-sphere gas. We will study how energy, chemical potential and mean square radius change as we vary the number of particles and the anisotropy of the trap. Particulary, we will focus on the differences between GP and MGP. We will also study the aspect ratio of the system in a deformed trap to compare with the analytic solution of the noninteracting anisotropic harmonic oscillator and the models that describe the system in a strongly repulsive case.

## II. THEORETICAL BACKGROUND

### A. Gross-Pitaevskii equation

Let us consider $N$ bosons in a trap of the form $V_{\text{trap}} = \frac{m}{2}(\omega_\perp^2(x^2+y^2)+\omega_z^2 z^2)$, where $\omega_\perp$ and $\omega_z$ are the two angular frequencies, in equilibrium ideally at temperature $T = 0K$.

Let us now consider an expansion parameter $x = na^3$ that leads us to the following low-density expansion for the energy density

$$\frac{E}{V} = \frac{2\pi n^2 a\hbar^2}{m}\left[1+\frac{128}{15}\left(\frac{na^3}{\pi}\right)^{\frac{1}{2}}+\mathrm{O}(na^3)\right], \quad (1)$$

where $n$ is the density and $a$ the $s$-wave scattering length. The energy functional for the GP equation in the LDA framework is obtained by keeping only the first term in the expansion (1)

$$E_{GP}[\psi(\mathbf{r})] = \int d\mathbf{r}\left[\frac{\hbar^2}{2m}|\nabla\psi(\mathbf{r})|^2 + V_{\text{trap}}(\mathbf{r})|\psi(\mathbf{r})|^2 + \frac{2\pi\hbar^2 a}{m}|\psi(\mathbf{r})|^4\right]. \quad (2)$$

Performing a functional variation in $|\psi(\mathbf{r})|$ we obtain the GP equation

$$\left[-\frac{\hbar^2\nabla^2}{2m}+V_{\text{trap}}(\mathbf{r})+\frac{4\pi\hbar^2 a}{m}|\psi(\mathbf{r})|^2\right]\psi(\mathbf{r}) = \mu\psi(\mathbf{r}), \quad (3)$$

where $\mu$ is the chemical potential and $\psi(\mathbf{r})$ is the wave function normalized to the number of atoms $N$

$$\int d\mathbf{r}|\psi(\mathbf{r})|^2 = N. \quad (4)$$

To obtain the MGP equation we need to consider the next term of the expansion (1). Doing the previous process with the second term we obtain the MGP energy functional

$$E_{MGP}[\psi(\mathbf{r})] = \int d\mathbf{r}\left[\frac{\hbar^2}{2m}|\nabla\psi(\mathbf{r})|^2 + V_{\text{trap}}(\mathbf{r})|\psi(\mathbf{r})|^2 + \frac{2\pi\hbar^2 a}{m}|\psi(\mathbf{r})|^4\left(1+\frac{32a^{\frac{3}{2}}}{3\pi^{\frac{1}{2}}}|\psi(\mathbf{r})|\right)\right] \quad (5)$$

and the corresponding MGP equation

$$\left[-\frac{\hbar^2\nabla^2}{2m}+V_{\text{trap}}(\mathbf{r})+\frac{4\pi\hbar^2 a}{m}|\psi(\mathbf{r})|^2\right.$$

| N | E | $\mu$ | $E_{\text{h.o.}}$ | $E_1$ | $E_{\text{kin}}$ | $< r^2 >$ |
|---|---|---|---|---|---|---|
| 1 | 1.500 | 1.500 | 0.750 | 0.000 | 0.750 | 1.500 |
| 10 | 1.899 | 2.213 | 1.028 | 0.313 | 0.557 | 2.057 |
| $10^2$ | 3.494 | 4.635 | 2.032 | 1.141 | 0.320 | 4.065 |
| $10^3$ | 8.051 | 11.144 | 4.797 | 3.086 | 0.168 | 9.594 |
| $10^4$ | 19.842 | 27.712 | 11.894 | 7.869 | 0.084 | 23.782 |
| $2 \times 10^4$ | 27.482 | 38.531 | 16.467 | 10.934 | 0.068 | 33.008 |

TABLE I: Energy, chemical potential, different contributions to the energy and mean square radius per particle of $N$ $^{87}$Rb atoms with scattering length $\bar{a} = 0.15155$ obtained with GP. All quantities are in h.o. units.

$$\left(1 + \frac{32a^{\frac{3}{2}}}{3\pi^{\frac{1}{2}}}|\psi(\mathbf{r})|\right)\Bigg]\psi(\mathbf{r}) = \mu\psi(\mathbf{r}), \tag{6}$$

From now on, to simplifly the notation we are going to use harmonic oscillator (h.o.) units for energy and length, defined as $\mathbf{r} = a_{\text{h.o.}}\bar{\mathbf{r}}$, $\bar{a} = a/a_{\text{h.o.}}$ and $\psi(\mathbf{r}) = \sqrt{N/a_{\text{h.o.}}^3}\psi_1(\bar{\mathbf{r}})$, where $a_{\text{h.o.}} = \sqrt{\hbar/m\omega}$ and $\psi_1(\bar{\mathbf{r}})$ is normalized to unity.

### B. Noninteracting model

In the noninteracting case the system is described by the wave function

$$\psi_1(\bar{\mathbf{r}}) = \lambda^{\frac{1}{4}}\pi^{-\frac{3}{4}}\exp[-\frac{1}{2}(\bar{x}^2 + \bar{y}^2 + \lambda\bar{z}^2)]. \tag{7}$$

Where $\lambda = \omega_z/\omega_\perp$ is the asymmetry parameter. The chemical potential coincides with the energy per particle, which is $(1+\lambda/2)$. The wave function has different transverse and vertical widths. In particular we have $\langle\bar{x}^2\rangle = 1/2$ and $\langle\bar{z}^2\rangle = 1/(2\lambda)$. We define the aspect ratio as

$$\sqrt{\langle\bar{x}^2\rangle/\langle\bar{z}^2\rangle} = \sqrt{\lambda}, \tag{8}$$

which characterizes the anisotropy of the distribution.

### C. Thomas-Fermi limit

A particulary useful and simple limit of the GP equation is obtained when we neglect the kinetic energy in front of the potential and interaction energies. This is the Thomas-Fermi (TF) limit. Applying this limit to the GP equation we obtain

$$\left[\frac{1}{2}(\bar{x}^2 + \bar{y}^2 + \lambda^2\bar{z}^2) + 4\pi\bar{a}N|\psi_1(\bar{\mathbf{r}})|^2\right]\psi_1(\bar{\mathbf{r}}) = \mu\psi_1(\bar{\mathbf{r}}). \tag{9}$$

Equation that can be solved for $\psi_1(\bar{\mathbf{r}})$ giving a density of $\rho(\bar{\mathbf{r}}) = |\psi_1(\bar{\mathbf{r}})|^2$

$$N\rho(\bar{\mathbf{r}}) = \frac{1}{4\pi\bar{a}}\left[\mu - \frac{1}{2}(\bar{x}^2 + \bar{y}^2 + \lambda^2\bar{z}^2)\right]. \tag{10}$$

From (9) we can conclude that the maximum radii of the system are $R_{\max_z} = \sqrt{2\mu}/\lambda$ and $R_{\max_{x-y}} = \sqrt{2\mu}$ for the $z$ axis and the $x-y$ axis respectively. The chemical potential in this limit normalizing the density to 1 is

$$\mu = \frac{1}{2}(15\bar{a}N\lambda)^{\frac{2}{5}}, \tag{11}$$

and the aspect ratio is

$$\sqrt{\langle\bar{x}^2\rangle/\langle\bar{z}^2\rangle} = \lambda. \tag{12}$$

In the isotropic GP case ($\lambda = 1$) the energy and mean square radius of the system can be expressed in terms of the chemical potential as $E = \frac{5}{7}\mu$ and $\langle r^2\rangle = \frac{6}{7}\mu$.

For the MGP equation the corresponding TF limit gives

$$\left[\frac{1}{2}(\bar{x}^2 + \bar{y}^2 + \lambda^2\bar{z}^2) + 4\pi\bar{a}N|\psi_1(\bar{\mathbf{r}})|^2 + 5\pi^{\frac{1}{2}}\bar{a}^{\frac{5}{2}}N^{\frac{3}{2}}\frac{128}{15}|\psi_1(\bar{\mathbf{r}})|^3\right]\psi_1(\bar{\mathbf{r}}) = \mu\psi_1(\bar{\mathbf{r}}). \tag{13}$$

In this case $\psi_1(\bar{\mathbf{r}})$ cannot be analytically obtained. The TF limit is determined numerically.

### D. Virial theorem

A virial theorem exists both for GP and MGP results which provides a particulary simple relation between the average kinetic, potential and interaction energies per particle

$$2E_{\text{kin}} - 2E_{\text{h.o.}} + 3E_1 + \frac{9}{2}E_2 = 0, \tag{14}$$

where $E_{\text{kin}}$ is the average kinetic energy, $E_{\text{h.o.}}$ the average harmonic oscillator energy, $E_1$ the average interaction energy due to the first term of the expansion (1) and $E_2$ the

| N | E | $\mu$ | $E_{\text{h.o.}}$ | $E_1$ | $E_{\text{kin}}$ | $< r^2 >$ | $E_2$ |
|---|---|---|---|---|---|---|---|
| 1 | 1.500 | 1.500 | 0.750 | 0.000 | 0.750 | 1.500 | 0.000 |
| 10 | 1.955 | 2.319 | 1.082 | 0.287 | 0.534 | 2.163 | 0.046 |
| $10^2$ | 3.825 | 5.175 | 2.321 | 0.924 | 0.295 | 4.642 | 0.281 |
| $10^3$ | 9.359 | 13.201 | 5.901 | 2.254 | 0.151 | 11.801 | 1.052 |
| $10^4$ | 24.601 | 35.091 | 15.821 | 5.129 | 0.075 | 31.633 | 3.576 |
| $2 \times 10^4$ | 33.095 | 47.312 | 21.382 | 6.527 | 0.036 | 42.637 | 5.126 |

TABLE II: Energy, chemical potential, different contributions to the energy and mean square radius per particle of $N$ $^{87}$Rb atoms with scattering length $\bar{a} = 0.15155$ obtained with MGP. All quantities are in h.o. units.

average interaction energy due to the second one. The definitions of $E_1$ and $E_2$ are

$$E_1 = 2\pi\bar{a}\int dr|\psi_1(\bar{\mathbf{r}})|^4, \tag{15}$$

$$E_2 = 2\pi\bar{a}\frac{128}{15}\left(\frac{\bar{a}^3}{\pi}\right)^{\frac{1}{2}}\int dr|\psi_1(\bar{\mathbf{r}})|^5. \tag{16}$$

### E. Numerical method

A numerical method to find the lowest energy state of a given hamiltonian $\hat{H}$ is the imaginary time step method, described for instance in Ref [5]. Let us consider the basis of non-degenerate eigenfunctions of $\hat{H}$ that fulfill $\hat{H}|\varphi_n\rangle = E_n|\varphi_n\rangle$, with $E_n$ the energy of the state $|\varphi_n\rangle$. We define the ground state energy $E_0$ as the lowest value of $E_n$.

We can also define a starting trial function $|\phi\rangle$ such that

$$|\phi\rangle = \sum_n c_n|\varphi_n\rangle. \tag{17}$$

The time-evolution of this state is governed by the Hamiltonian $\hat{H}$ through the unitary evolution operator $U(t) = e^{-i\hat{H}t/\hbar}$

$$|\phi(t)\rangle = e^{-i\hat{H}t/\hbar}|\phi(0)\rangle = \sum_n e^{-iE_nt/\hbar}c_n|\varphi_n\rangle. \tag{18}$$

The imaginary time step method consists in considering an imaginary time $t$ such that $\tau = it$ is real. However, this transformation gives a non-unitary operator $U(t)$, thus the norm will not be preserved. In the limit $\tau \to \infty$ only the $E_0$ contribution survives in the evolution of $|\phi\rangle$ thus

$$\lim_{\tau\to\infty}|\phi\rangle \propto c_0|\varphi_0\rangle. \tag{19}$$

To solve the loss of norm in the numerical iteration the algorithm has to be implemented using small time steps $\delta\tau$ and renormalizing after each step. At first order

$$|\phi(\tau+\Delta\tau)\rangle \simeq \left(1 - \frac{\hat{H}\delta\tau}{\hbar}\right)|\phi(\tau)\rangle \tag{20}$$

When this process is repeated a large enough number of times $|\phi_n\rangle$ converges to the ground state $|\varphi_0\rangle$, provided $c_0 \neq 0$. An important point to take into account is the value of $\delta\tau$. It has to be small enough to guarantee the convergence of the algorithm, but large enough to make it efficient.

## III. ISOTROPIC CASE

### A. Gross-Pitaevskii results

In this section we concentrate on the isotropic case and compare the GP and the MGP results. We have performed calculations with $N$ particles ranging from 1 to $2\times10^4$ with $\bar{a} = 0.15155$ in h.o. units using the GP equation. The energies, chemical potential and mean square radius per particle are reported in Table I. For one particle we obtain the harmonic oscillator, where kinetic energy and harmonic oscillator potential are equal and the interaction energy is zero. For $2 \times 10^4$ particles the kinetic energy decreases and the interaction potential becomes a significant part of the energy.

In Fig. 1 we have plotted the different energies of the system and the mean square radius per particle rescaled to the chemical potential. There we see that as $N$ increases the scaled energy and mean square radius tend to the analytic limits 5/7 and 6/7 respectively. For $2 \times 10^4$ particles we find relative differences between our results and the TF limit of 0.15% for energy and 0.05% for mean square radius.

### B. Modified Gross-Pitaevskii results

To study the modified isotropic case we have repeated the previous process using the MGP equation performing calculations for the same number of particles. The energies, chemical potential and mean square radius per particle are reported in Table II. Now, there is another energy, called $E_2$ due to the second term of (1).

In the large $N$ limit the MGP results approach, as expected, to the corresponding TF limit. The numerical

| | GP−1 | | | GP−2 | | | MGP−2 | | |
|---|---|---|---|---|---|---|---|---|---|
| N | $\mu$ | $\sqrt{\langle\bar{x}^2\rangle}$ | $\sqrt{\langle\bar{z}^2\rangle}$ | $\mu$ | $\sqrt{\langle\bar{x}^2\rangle}$ | $\sqrt{\langle\bar{z}^2\rangle}$ | $\mu$ | $\sqrt{\langle\bar{x}^2\rangle}$ | $\sqrt{\langle\bar{z}^2\rangle}$ |
| 1 | 2.414 | 0.707 | 0.420 | 2.414 | 0.707 | 0.420 | 2.414 | 0.707 | 0.420 |
| $10^2$ | 2.864 | 0.827 | 0.436 | 7.175 | 1.370 | 0.566 | 8.147 | 1.493 | 0.599 |
| $2\times10^2$ | 3.196 | 0.874 | 0.446 | 9.207 | 1.571 | 0.620 | 10.671 | 1.731 | 0.668 |
| $5\times10^2$ | 3.922 | 0.976 | 0.470 | 12.989 | 1.888 | 0.714 | 15.465 | 2.112 | 0.785 |
| $10^3$ | 4.760 | 1.088 | 0.495 | 16.967 | 2.172 | 0.803 | 20.626 | 2.456 | 0.897 |
| $2\times10^3$ | 5.927 | 1.231 | 0.530 | 22.246 | 2.498 | 0.910 | 27.627 | 2.857 | 1.031 |
| $5\times10^3$ | 8.146 | 1.469 | 0.592 | 31.937 | 3.004 | 1.080 | 40.847 | 3.491 | 1.248 |
| $10^4$ | 10.511 | 1.687 | 0.654 | 42.051 | 3.454 | 1.234 | 55.055 | 4.065 | 1.447 |
| $1.5\times10^4$ | 12.248 | 1.830 | 0.697 | 49.412 | 3.747 | 1.335 | 65.616 | 4.444 | 1.579 |
| $2\times10^4$ | 13.671 | 1.939 | 0.730 | 55.411 | 3.970 | 1.413 | 74.343 | 4.735 | 1.681 |

TABLE III: Chemical potentials and aspect ratios scaled to the number of particles in a deformed trap for GP and MGP in h.o. units. The index 1 corresponds to particles with a scattering length $\bar{a}_1 = 0.00433$ and the 2 to particles with a scattering length $\bar{a}_2 = 0.15155$.

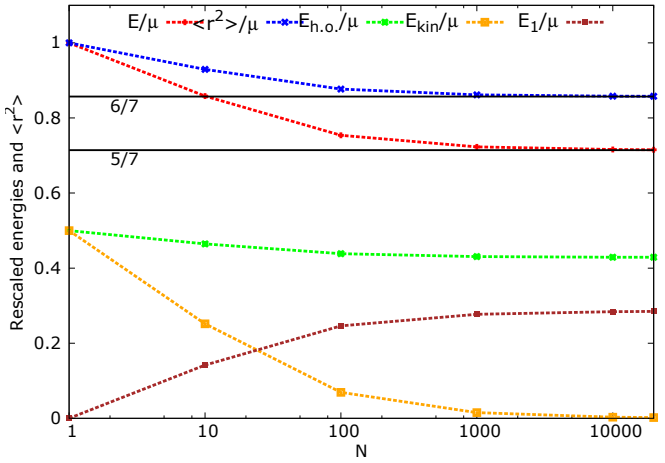


FIG. 1: Energies and mean square radius per particle scaled to the chemical potential for different number of particles using GP equation with $\bar{a} = 0.15155$ in an isotropic trap compared with the TF limit.

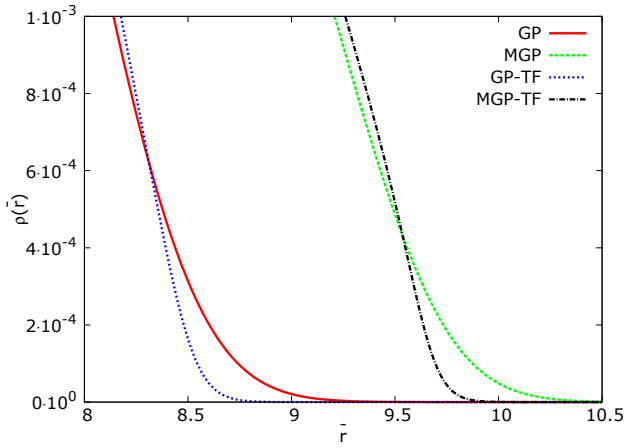


FIG. 2: Density tails of a $2 \times 10^4$ particle system using GP, MGP and its TF limits at the border of the system with a scattering length of 0.15155 in an isotropic trap in h.o. units.

TF limit is 0.6988 for energy and 0.9038 for mean square radius, finding relative differences between this limit and the scaled results for $2 \times 10^4$ particles of 0.1% and 0.29% respectively.

Finally, we compare the densities of the systems obtained with GP and MGP and their TF limits in Fig 2. In the TF limit, the system will have a maximum radius of $R^{\rm GP}_{\rm max-TF} = 8.7$ for GP and $R^{\rm MGP}_{\rm max-TF} = 9.7$ for MGP. An important difference between the GP and MGP results and their corresponding TF limits is found in the density tails at the edge of the cloud. In the TF limit the density has a sharp edge, while in the GP and MGP the density decreases smoothly on the edge. Despite that the system in the TF limit should have (at least in the GP case) a snappish end we see a small meniscus. This is because these limits are calculated numerically and is difficult to reach the exact parabolic function.

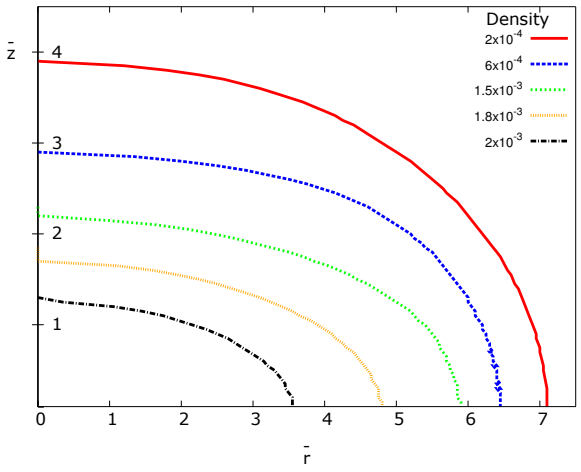


FIG. 3: Density level curves of 5000 $^{87}$Rb particles with scattering length 0.15155 obtained with MGP in a trap with deformation $\lambda = \sqrt{8}$. All quantities are in h.o. units.

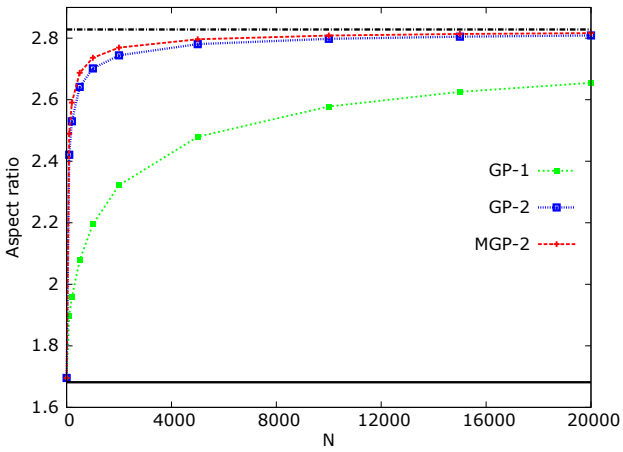


FIG. 4: Comparison of the aspect ratio as a function of the number of particles for different scattering lengths $\bar{a}_1$ and $\bar{a}_2$. The solid and dotted dashed horizontal lines correspond to the noninteracting and TF limit respectively.

## IV. ANISOTROPIC CASE

In this section we consider an anisotropic cylindrical trap with an asymmetry parameter $\lambda = \sqrt{8}$. We have performed calculations from 1 particle to $2\times10^4$ particles and for two different scattering lengths, $\bar{a}_1 = 0.00433$ and $\bar{a}_2 = 0.15155$ using GP. We have also done the same study with MGP but only for the $\bar{a}_2$ case, due to the fact that for a small scattering length like $\bar{a}_1$ the differences between GP and MGP are negligible.

In Fig. 3 we show the density level curves of 5000 particles with a scattering length $\bar{a}_2$ and $\lambda = \sqrt{8}$ with MGP. Here we observe that the system expands more in $\bar{r}$ than in $\bar{z}$. This is because the repulsion bewteen particles tends to lower the central density and expand the atom cloud towards regions where the trapping potential is less stiff.

In Fig. 4 we have plotted the aspect ratio for different number of particles using $\bar{a}_1$ and $\bar{a}_2$. The results are reported on Table III. For the noninteracting limit we obtain $\sqrt{\lambda}$ (Eq. 8). For $2 \times 10^4$ particles using GP we obtain $\lambda$ (Eq. 12), arriving faster for bigger scattering lengths. We have also studied the MGP aspect ratio, which is larger than for GP. Although the values of $\sqrt{\langle\bar{x}^2\rangle}$ and $\sqrt{\langle\bar{z}^2\rangle}$ change considerably respect to the GP ones, the aspect ratio is much less affected. The asymptotic value, which corresponds to TF, is $\sqrt{8}$ for GP and 2.841 for MGP. However, the MGP aspect ratio as a function of $N$ reaches to the asymptotic value much faster than the GP one.

## V. CONCLUSIONS

In this degree thesis we have studied a trapped diluted $^{87}$Rb gas with a scattering length $\bar{a}$ using GP and MGP equation and their TF limits for a finite number of particles in an isotropic trap. After solving the equation for different number of particles we have concluded that for a large enough number of particles the results for GP fit with the TF limit. For MGP we have found that for a large enough number of particles our results also fit with the proper numerical TF limit.

We have also studied the behaviour of a trapped diluted $^{87}$Rb ultracold system with a deformation $\lambda$ in the GP and MGP cases for two scattering lengths, $\bar{a}_1$ and $\bar{a}_2$ solving the equations for different number of particles. For the noninteracting case we obtain an aspect ratio of $\sqrt{\lambda}$. For the strong repulsive limit using GP for a finite number of particles we have found that the aspect ratio tends to $\lambda$, reaching faster the limit for larger scattering lengths. For MGP the strong repulsive limit should be calculated numerically obtaining a value slightly larger than the actual deformation of the trap. This is because in MGP there is an additional contribution to the energy, which is positive, i.e., repulsive, that makes a the ratio larger.

We have found that the deformation of the gas cloud is not the same as the one of the trap. The atomic system deformation depends on the number of particles. In the noninteracting limit the kinetic energy is a significant part of the total energy, which partially compensates the anisotropy of our trap. In the strong repulsive GP limit, the kinetic energy does not contribute to the total energy, obtaining the same deformation as the one of the trap. However, for MGP we have found that this anisotropy is slightly higher than the trap deformation due to the larger repulsion between particles.

### Acknowledgments

I would like to thank Bruno Juliá-Díaz and Artur Polls for his invaluable guidance during the elaboration of the ideas here exposed, and for giving me the opportunity to experience the thrilling field of condensed matter. Also thank my parents and friends for their help and support, special thanks to Marcos Pou that, from other place, has been helping and inspiring me all this time.

[1] E. Lipparini, "Modern Many-Particle Physics: Atomic Gases, Quantum Dots and Quantum Fluids", Singapore: World Scientific (2003).
[2] J.K. Nielsen, J. Mur-Petit, M. Guilleumas, M. Hjorth-Jensen, A. Polls, "Vortices in atomic Bose-Einstein condensates in the large-gas-parameter region", Phys. Rev. A **71**, 053610 (2005).
[3] A. Fabrocini, A. Polls, "Beyond the Gross-Pitaevskii approximation: Local density versus correlated basis approach for trapped bosons", Phys. Rev. A **60**, 2319 (1999).
[4] F. Dalfovo, S. Stringari, "Bosons in anisotropic traps: Ground state and vortices", Phys. Rev. A **53**, 2477 (1996).
[5] M. Melé, "Josephson effect in multicomponent Bose-Einstein condensates", PhD thesis, University of Barcelona (2013).